

ACOUSTIC EMISSION CHARACTERIZATION OF SINGLE AND DUAL FIBER REINFORCED METAL MATRIX COMPOSITES

Joon-Hyun Lee, Won-Jin Sung

School of Mechanical Engineering
Pusan National University
Pusan 609-735, Korea

INTRODUCTION

Interfacial shear strength (IFSS) between fiber and matrix is one of the most important factors in characterizing the mechanical properties of fiber reinforced composites. If the IFSS is too low, it's hard to expect the performance of reinforcing fibers in composites, whereas if the IFSS is too high, there is a decrease in fracture toughness of composites because of the poor resistance to the stress crack propagation. Hence, it is necessary that the IFSS should be determined via the optimization rather than the maximization for the purpose. Several micro-mechanical techniques were proposed for measuring IFSS in composites. Some of the most frequently used techniques include the single fiber pull-out test[1], the single fiber composite (SFC) test[2], and micro-indentation method[3]. Among them, the SFC test, originally proposed by Kelly and Tyson[4], has received a lot of attention both as a diagnostic for fiber/matrix adhesion and as a simple composite system composed of the elastic fiber imbedded in a plastic matrix, Kelly and Tyson showed that the critical fragment length l_c is given by

$$l_c = \frac{d\sigma_f}{2\tau_i} \quad (1)$$

where d is the fiber diameter, τ_i is the IFSS, σ_f is the fiber fracture stress.

In this paper, some results have been introduced to understand the characteristics of micro-failure mechanism and interfacial shear strength between fiber and matrix for metal matrix composite(MMC), which were obtained from the tensile test using the SFC and dual fiber composite(DFC) specimens with the aid of Acoustic Emission (AE) method.

MATERIALS AND EXPERIMENTAL PROCEDURES

In the present study SiC (Nicalon) and Boron fiber were used as reinforcement and Al6061 as matrix, respectively. The mechanical properties of each fiber are represented in Table 1. Four kinds of dog-one shaped specimens were prepared by squeeze casting technique for the SFC and DFC test, Al6061 matrix specimen, single SiC fiber reinforced Al6061 composite specimen, single Boron fiber reinforced Al6061 composite specimen and dual (SiC, Boron) fibers reinforced Al6061 composite specimen. Fig.1 represents dimensions of DFC test specimens. Instruments for SFC and DFC tests were represented in Fig. 2. SFC test was made with a crosshead speed of 0.005mm/min using

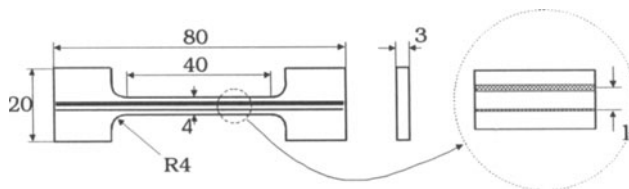


Fig. 1. Dimensions of DFC test specimens

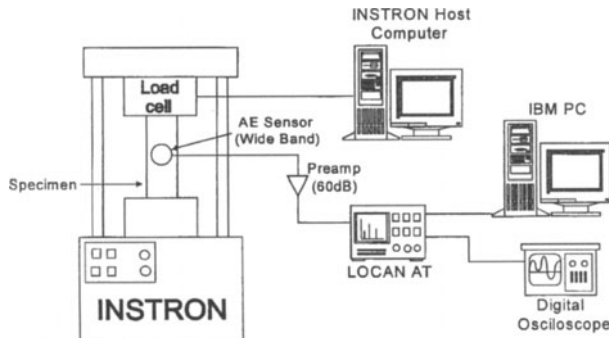


Fig. 2. Schematic diagram of instrumentation for SFC and DFC test

Table 1. Mechanical properties of fibers

| | SiC | Boron |
|-----------------------------|-------|-------|
| Density(g/cm ³) | 2.6 | 2.6 |
| Diameter(μm) | 10~20 | 150 |
| Modulus(GPa) | 180 | 385 |
| Strength(GPa) at 20 °C | 2 | 3.8 |
| at 1400 °C | 0.5 | - |

INSTRON. At room temperature progressive breaking of the fiber was detected with AE using a wide band AE sensor(PAC) which was attached to the center of the specimens. The sensor output was amplified by 60dB at preamplifier and then sent into AE signal processing unit, LOCAN AT, where AE parameters were analyzed. In addition, frequency analysis of AE waveforms by Fast Fourier Transformation(FFT) was used to characterize the failure mode. During SFC and DFC tests stress was increased until no further fiber breakage were observed. After each test the one side of MMC specimen was polished and the fiber fragments were observed via optical microscope and ultrasonic C-scan technique.

RESULTS AND DISCUSSIONS

Characteristic of AE signal

In the present study, SFC and DFC test for four different specimens, namely, Al6061 matrix, SiC/Al6061 composite, Boron/Al6061 composite and DFC composite specimen, were carried out to evaluate the IFSS between fiber and matrix and to characterize microscopic failure mode. Special attention was paid to on-line monitoring of fiber breakage during the test using AE technique. Fig.3 showed Time vs. load and AE events for Al6061 matrix and three different MMC specimens,

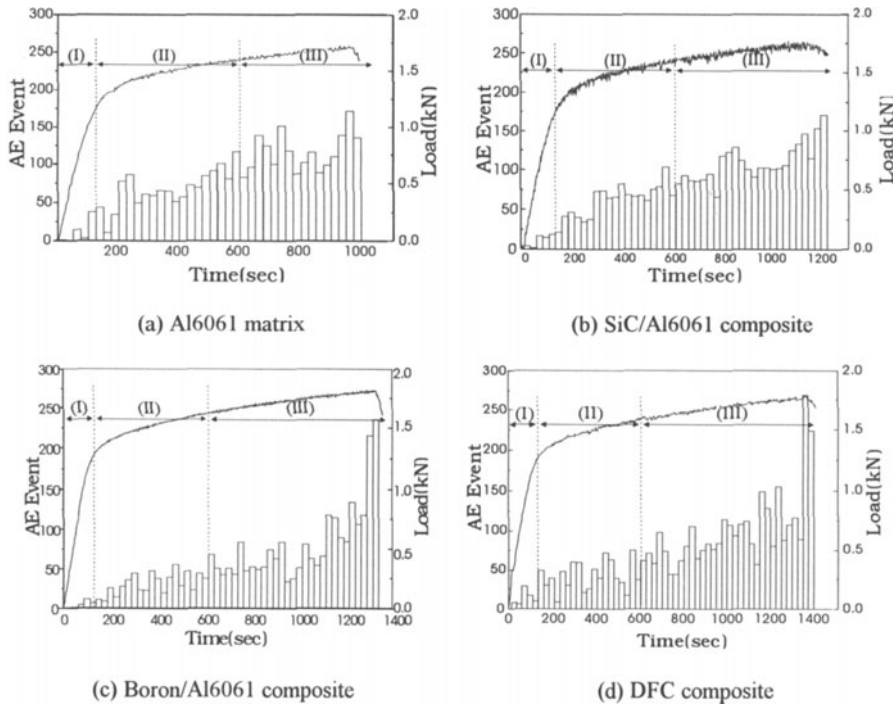


Fig. 3. AE events and Load vs. Time

respectively. As shown in Fig.3, AE events increased with load for all specimens and the characteristics of AE events were divided by three groups in all specimens ; that is, the stage(I) of the elastic deformation (0 ~ 150(sec)) ; the stage (II) of the former plastic deformation (150 ~ 600(sec)) ; the stage (III) of the latter plastic deformation (after 600(sec)). The Al6061 matrix specimen shown in Fig.3(a) indicated low AE events occurrence in the stage(I) of the elastic deformation because the occurrence and growing rate of micro-cracks were low and deformation energy could not be emitted but stored in the material. In the stage(II), AE events increased gradually because of the emission of deformation energy by the micro-cracks due to stress concentration source such as small amount of the porosity and inclusions in the materials. In the stage(III), AE events relatively increased highly compared with stage(II). This is because of the increase of micro-cracks with which occurred newly and the link-up of each micro-crack. For MMC specimen shown in Fig.3(b), (c), (d), AE event rate was relatively low in the stage(I) of the elastic deformation but from plastic deformation stage(II) AE event rate increased abruptly. While AE events in stage(II) were due to micro-cracks in the matrix and partial fiber breakage, AE events in stage(III) were due to growth of micro-crack by linkage and further fiber breakage.

Fig.4 showed the relationships between AE amplitude and AE events measured. Since the characteristics of electrical noise of AE signal was investigated in pre-test procedure, appropriate threshold level was set to eliminate noise signals. Thus, AE signals below threshold level of 50 dB were not detected. While no signals above 77dB were observed for Al6061 matrix specimen, the amplitude ranging from 77~100dB was distributed for SFC and DFC specimens. This is because there were more defects and AE sources by fiber breakage in MMC specimen than in Al6061 matrix. It has been reported that AE signals due to matrix cracking showed the lower amplitude signal than those due to fiber breakage in composite materials[5]~[6]. Thus the signals with 77~100dB in amplitude were due to the fiber breakage and partially debonding. AE amplitude distribution for the

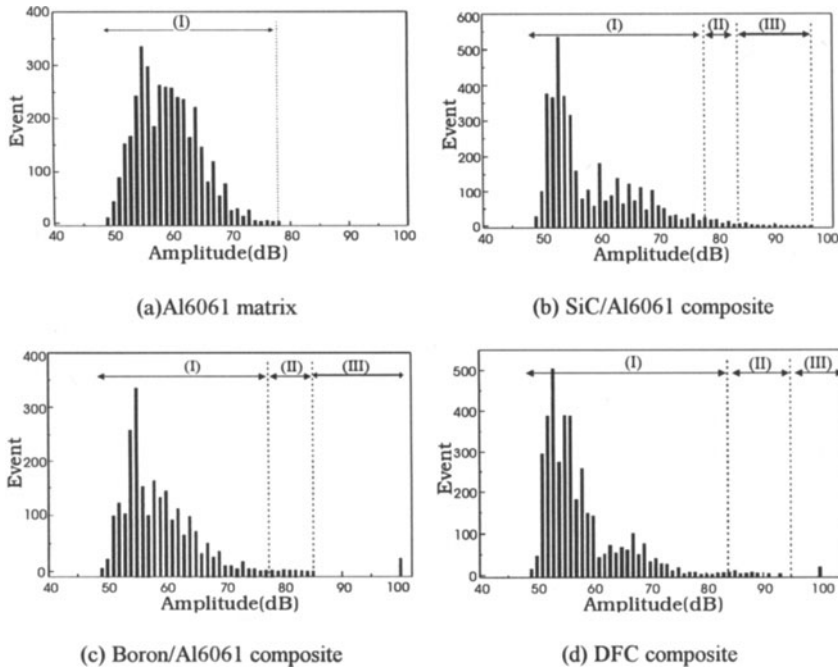


Fig. 4. AE events vs. Amplitude

Boron/Al6061 composite could be classified into three stages shown in Fig.4(c). It was obviously found that the stage(II), (III) which was not observed for Al6061 matrix specimen were mainly due to the effect of fiber in matrix. Thus, the signals of the higher AE amplitude observed in stage(III) were due to the Boron fiber breakage and stage(II) not observed for Al6061 matrix could be considered due to debonding between fiber and matrix. Similar results were also observed for SiC/Al6061 composite specimen as shown in Fig.4(b), but AE signals coming from SiC fiber breakage wider distribution showed relatively, that is, ranging from 84~95dB in amplitude. After understanding the AE characteristic in each AE source such as matrix cracking, debonding and fiber breakage through the SFC test above, the DFC test for specimens reinforced by two different fibers was done. As shown in Fig.4(d), in the DFC composite AE signals generated in each AE source could be classified into three groups as follows: stage(I) due to matrix cracking and debonding, stage(II) due to SiC fiber breakage, stage(III) due to Boron fiber breakage.

Fig.5 showed the relationship between AE amplitude and energy for both Al6061 matrix and MMC specimens. For Al6061 matrix specimen AE signals were mostly distributed by both 77dB in amplitude and 80dB in energy. Meanwhile, higher AE energy associated with fiber breakage was clearly observed from MMC specimens shown in Fig.5(b),(c),(d). As shown in Fig.5(c), AE energy due to Boron fiber breakage is higher than that due to SiC fiber breakage. This is mainly attributed to effect of diameter size shown in Table 1. If we look at relationship between AE energy and duration time for four different specimens, similar characteristics were also observed as shown in Fig.6. It was found in Fig.6(b) that AE duration time due to SiC fiber breakage was mainly distributed to the range of 260~600(μ sec), but much longer duration time range from 1500~3000(μ sec) was observed for Boron fiber breakage shown in Fig.6(d). Consequently, AE Signals due to fiber breakage have higher energy and longer duration time than those associated with matrix cracking. It was also pointed out that AE amplitude and duration time versus AE energy were more useful parameters to distinguish AE signals corresponding to fiber breakage and matrix

cracking, respectively. Based on the characteristics of AE signals we obtained, AE signals corresponding to each failure mechanism of MMC could be classified in Table 2.

Table 2. Classification of AE signals due to failure mechanism of MMC

| | Matrix cracking | Debonding | SiC fiber breakage | Boron fiber breakage |
|------------------------|-----------------|-----------|--------------------|----------------------|
| AE amplitude(dB) | ~77 | ~84 | 84~95 | 100 |
| AE energy(dB) | ~80 | ~120 | 120~250 | 750~1400 |
| AE duration time(μsec) | ~225 | ~260 | 260~600 | 1500~3000 |

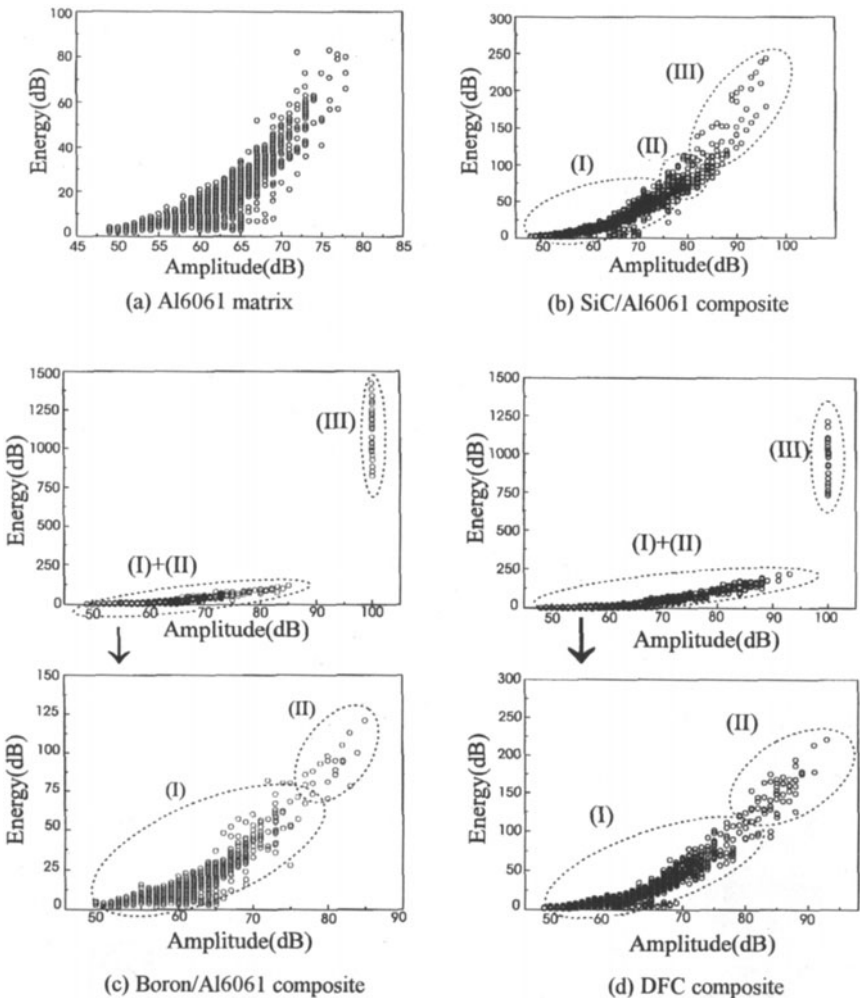


Fig. 5. Amplitude vs. AE energy

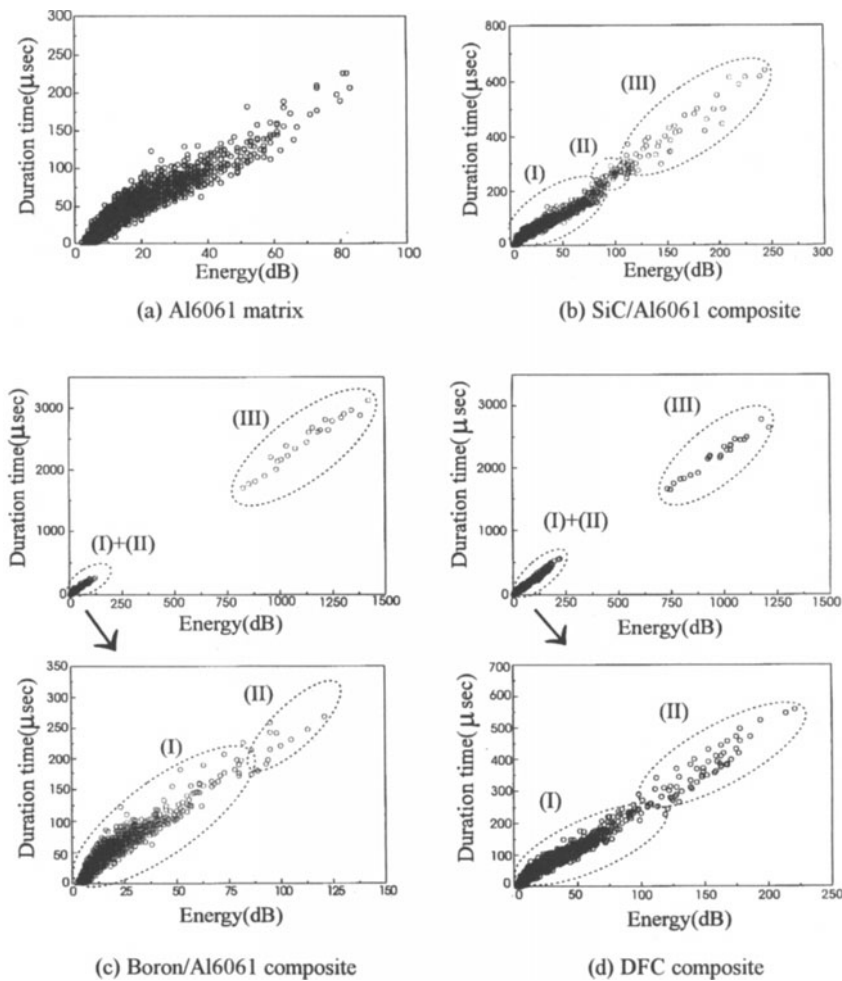


Fig. 6. AE energy vs. Duration time

Fig.7 showed the typical AE waveforms corresponding to each micro-failure process and their FFT spectrum from DFC test. As shown in Fig.7, the waveform associated with fiber breakage has the high amplitude above 8V and long duration time above 500μs, whereas the waveform during matrix cracking has the amplitude of lower voltage and shorter duration time of 200μs. For both matrix and fiber breakage, FFT results showed characteristic peak frequency at about 240kHz but the magnitude of frequency of fiber breakage was higher, especially for Boron fiber breakage than for matrix cracking.

Evaluation of Interfacial Shear Strength

It is well recognized that metal matrix composite exhibited has more complicate failure mechanisms than in PMC. This is because MMC contains usually more intrinsic defects in material such as inclusion, porosity etc., which might be caused during the fabrication process of MMC. Thus it is not so easy to distinguish AE signal associated with fiber breakage from the other AE signals in MMC. In this study, AE signals corresponding to fiber breakage could be determined by comparing

the characteristic of AE signals between MMC specimen and matrix specimen. It could be seen in this over 84dB were associated with the fiber breakages from the characterization of the AE signals in Fig.4~Fig.7. In order to verify the AE signal corresponding to the fiber breakage in MMC, the specimen after the SFC, DFC tests was carefully polished to observe the fiber breakage by optical microscope and ultrasonic C-scan. Fig.8 indicated the typical example of macrograph showing the multiple fiber breakage in MMC. The coincidence between the number of fiber breakage by AE signal characterization and by both ultrasonic C-scan and optical microscope was observed. Based on

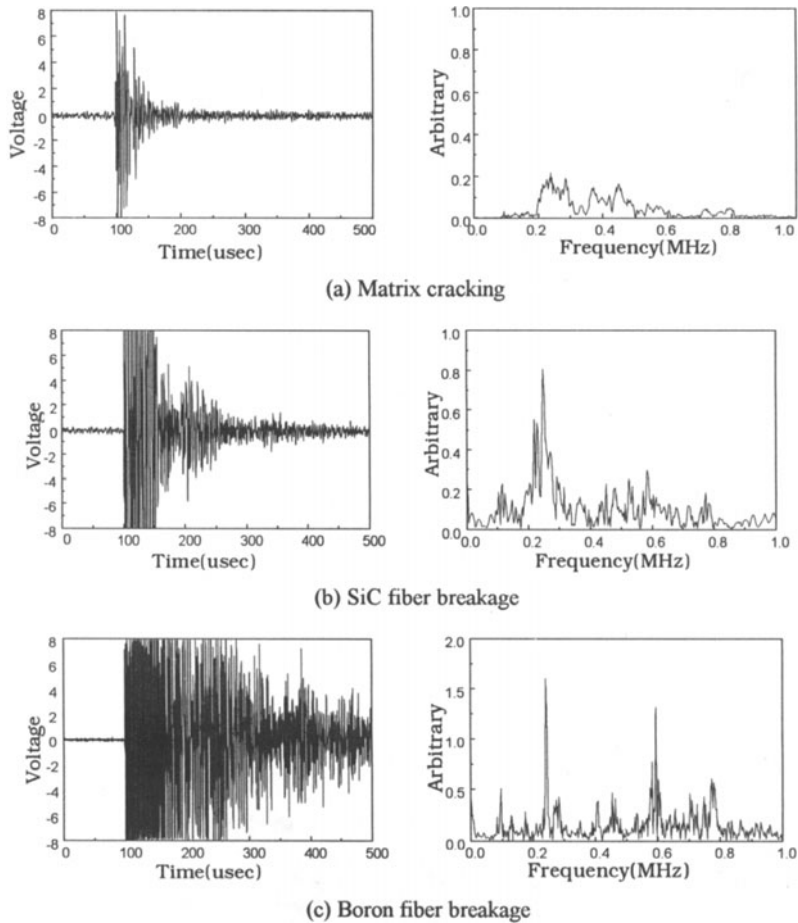


Fig. 7. AE waveforms and their FFT spectrums from DFC test

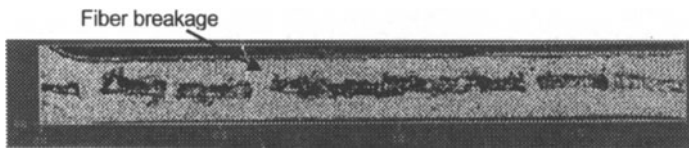


Fig. 8. Typical appearance of fiber breakage observed from ultrasonic C-scan.

the number of fiber breakage measured from the experiment, the average critical fiber fragmentation length was determined as shown in Table. 3, and by using these average critical fiber fragmentation length, IFSS could be calculated from Eq.(1) as listed in Table. 4. Thus AE method could be correlated reliably to the IFSS via SFC and DFC test.

Table 3. Average critical fiber fragmentation length from AE

| | SiC/Al6061 | Boron/Al6061 | Dual Fiber Composite | |
|---|------------|--------------|----------------------|-------------|
| | | | SiC fiber | Boron fiber |
| Gage length (mm) | 40 | 40 | 40 | 40 |
| Fiber breakage | 54 | 23 | 51 | 21 |
| Average critical fiber fragmentation length(mm) | 0.727 | 1.739 | 0.783 | 1.905 |

Table 4. Calculation of IFSS for SFC and DFC specimens

| Material | | σ_f (GPa) | $d(\mu\text{m})$ | l_c (mm) | τ_i (MPa) |
|----------------------|-------------|------------------|------------------|------------|----------------|
| SiC/Al6061 | | 2 | 15 | 0.727 | 20.6 |
| Boron/Al6061 | | 3.8 | 150 | 1.739 | 163.9 |
| Dual Fiber Composite | SiC fiber | 2 | 15 | 0.783 | 19.2 |
| | Boron Fiber | 3.8 | 150 | 1.905 | 149.6 |

CONCLUSIONS

In this study, we evaluated the IFSS of sigle and dual fiber reinforced MMC by fragmentation test with the aid of AE technique. It was found that three distinct failure mechanisms mainly associated with matrix cracking, debonding and fiber breakage could be observed from characteristics of AE signals from SFC and DFC specimens. AE amplitude and duration time vs. AE energy were useful parameters to distinguish AE signals corresponding to fiber breakage and matrix cracking, respectively. One-to-one correspondence between the AE event and fiber breakage for both SFC and DFC specimens can be established via Ultrasonic C-scan and Optical microscope, which gives us more reliable and convenient estimation of average critical fragmentation length to evaluate the IFSS.

REFERENCES

1. P. Lawrence, "Some Theoretical Considerations of Fiber Pull-Out from an Elastic Matrix", J. Mater. Sci., Vol. No.7, pp.1-6, 1972.
2. J. M. Park and Subramanian. R. V, "Interfacial Shear Strength and Durability Improvement by Monofilament and Polymeric Silanes in Basalt fiber/epoxy Signle-Filament Composite specimens", J. Adhesion Sci. & Technol., 5, 459, 1991.
3. D.B. Marshall, "An Introduction for Measuring Matrix-Fiber Friction Stress in Ceramic Composites", J. Am. Ceram. Soc., Vol.67, No.2, pp.259-260, 1984.
4. A. Kelly and W.R. Tyson, "Tensile Properties of Fiber Reinforced Materials: Copper/Tungsten and Copper/Molybdenum", J. Mech. Phys. Solids, Vol.13, pp.329-350, 1965.
5. J.M. Park and J.H. Lee, "Acoustic Emission Study of Micro-Failure Mechanism of Dual Basalt Filaments Reinforced Epoxy Composites", AECM-5, pp.240-249, Sundvall, Sweden, 1995.
6. J.M. Park, B. J. Son and J.H. Lee "Analysis of Interfacial Shear Strength and Micro-failure Mechanism of SiC fiber Reinforced Aluminum Composites using Single Fiber Composites and Acoustic Emission Techniques", ICCE-2, pp.617-618, 1996.